

Electron Transport Algorithms in the Integrated TIGER Series

Brian C. Franke, Ronald P. Kensek
RPSD 2018
Santa Fe, NM
August 26-31, 2018

Overview

- ITS Electron Transport Algorithms
 - Condensed History
 - Hybrid Continuous-Energy/Multigroup
 - Single Scatter (Based on LLNL Evaluated Data Library)
- Validation Comparisons
 - Lockwood Albedo (Uranium, 1 MeV – 30 keV)
 - Hanson Angular Scattering (Gold, 15.7 MeV)
 - Tabata Charge Deposition (Beryllium, 14.9 MeV)
 - McLaughlin Energy Deposition (Aluminum, 3 MeV)
 - Sanford Bremsstrahlung (Carbon, 750 keV)
 - McLaughlin Energy Deposition (Polystyrene, 100 keV)
 - Dolan Photoemission (Tantalum, 50 keV)
- Other Topics
 - Relaxation Radiation
 - Differential Operator for Sensitivities
 - Biasing with Electron Trapping

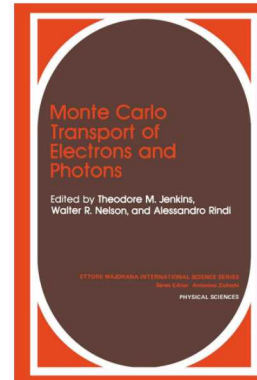
Condensed History

- Pre-computed energy-loss (step) and angular scattering (substep) distributions
- Goudsmit-Saunderson angular scattering
 - Screened Mott high-energy factorization above 256 keV
 - Fits to Riley data below 256 keV
 - Inelastic angular deflection based on $(Z+1)/Z$ correction
 - Jordan-Mack algorithm used for boundary crossings
- Energy loss from Blunck-Leisegang with Seltzer correction
 - Accounts for ionization and excitation energy loss
 - Option for per-substep straggling (per Hughes MCNP implementation)
- Bremsstrahlung events sampled from a Poisson distribution along each substep
 - Energy subtracted from primary electron
- Knock-on and relaxation events sampled along each substep
 - Sampled to preserve mean number of events
 - Not correlated with primary electron energy-loss
 - Relaxation cascade uses K and L shells, plus average N and M shells.

M. J. BERGER, "Monte Carlo Calculations of the Penetration and Diffusion of Fast Charged Particles," in B. ADLER, S. FERNBACH, and M. ROTENBERG, editors, "Methods in Computational Physics, Vol. 1," Academic Press, New York (1963).

T. M. JENKINS, W. R. NELSON, and A. RINDI, editors, "Monte Carlo transport of electrons and photons," Plenum Press, New York, Ettore Majorana international science series: Physical sciences (1988).

S. SELTZER, "Electron-Photon Monte Carlo Calculations: The ETRAN Code," *Appl. Radiat. Isot.*, 42, 10, 917–941 (1991).



Multigroup

- Group-to-group energy/angle scattering, within group angle scattering, CSDA.
- Angular scattering moments preserved through discrete-angle scattering
 - Screened Mott high-energy factorization above 256 keV
 - Fits to Riley data below 256 keV
 - Single discrete angle as a Fokker-Planck approximation
 - Inelastic angular deflection based on kinematics in group-to-group scattering
- Energy loss as Moller distribution and restricted stopping power
 - Accounts for ionization and excitation energy loss
 - Inelastic scattering events are distributed exponentially
 - Restricted stopping power is applied as a continuous-slowing-down approximation
- Bremsstrahlung, knock-on, and relaxation sampled as group-to-group scatters
 - Relaxation cascade uses K and L shells, plus average N and M shells
 - Secondaries and primaries are not correlated within the Monte Carlo simulation, but average behaviors are captured in the cross section data
- Multigroup cross sections can be inverted to enable adjoint simulations

J. E. MOREL, et al., Nucl. Sci. Eng., 124, 369–389 (1996).

L. J. LORENCE, JR., J. E. MOREL, and G. D. VALDEZ, SAND89-1685, Sandia National Laboratories (1989).

D. P. SLOAN, SAND83-7094, Sandia National Laboratories (1983).

J. A. HALBLEIB and J. E. MOREL, J. Comp. Phys., 34, 211 (1980).

Single Scatter

- Analog simulation using LLNL Evaluated Data Libraries
- Elastic angular scattering
 - Screened Mott high-energy factorization 10 MeV and above
 - Fit to Riley data for 1-256 keV
 - Isotropic at 10 eV
 - Screened Rutherford distribution for $\mu_0 \geq 0.999999$
- Inelastic electro-ionization scattering
 - Angular deflection based on particle kinematics
- Bremsstrahlung scattering
 - Energy subtracted from primary electron
 - Photon angular distribution based on the “simple-brems” model
- Knock-on and relaxation from ionization events
 - Detailed shell models for binding energies and relaxation cascade

S. PERKINS, D. CULLEN, and S. SELTZER, EEDL, UCRL-50400 Vol 31, LLNL (1991).

D. CULLEN, M. CHEN, J. HUBBELL, S. PERKINS, E. PLECHATY, J. RATHKOPF, and J. SCOFIELD, EPDL, UCRL-50400 Vol 6, LLNL (1989).

S. PERKINS, D. CULLEN, M. CHEN, J. HUBBELL, J. RATHKOPF, and J. SCOFIELD, EADL, UCRL-50400 Vol 30, LLNL (1991).

D. M. FLETCHER and B. C. FRANKE, in “Proc. M&C 2017,” Jeju, Korea (April 16-20 2017), American Nuclear Society (2017).

Lockwood Albedo

Electron beams incident on a thick slab of uranium

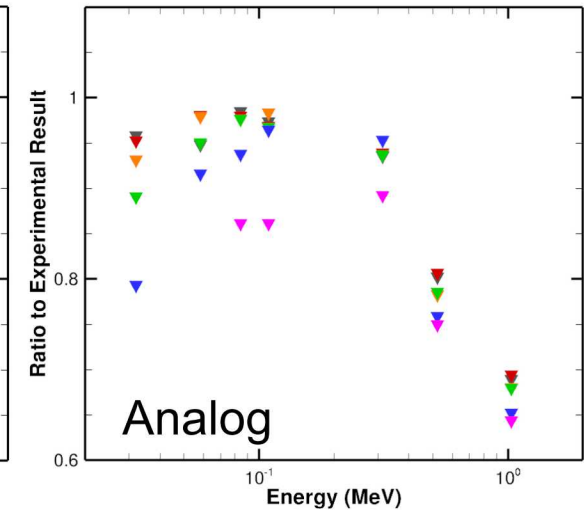
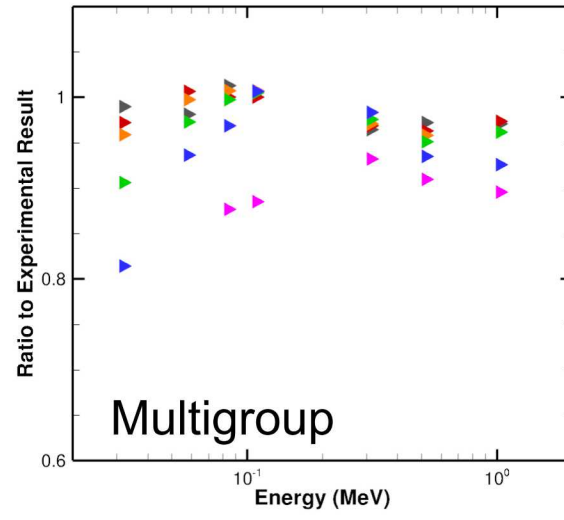
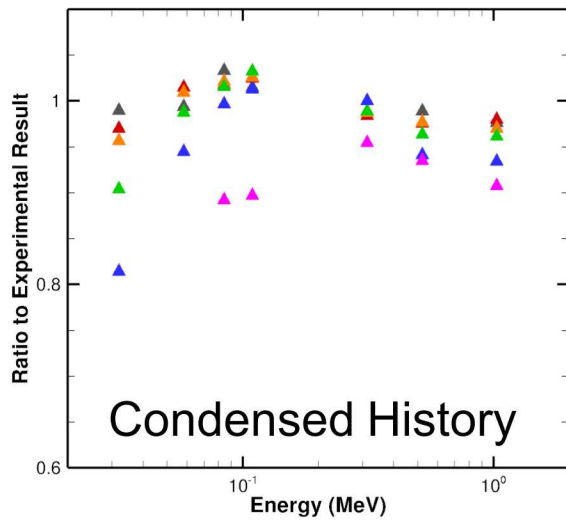
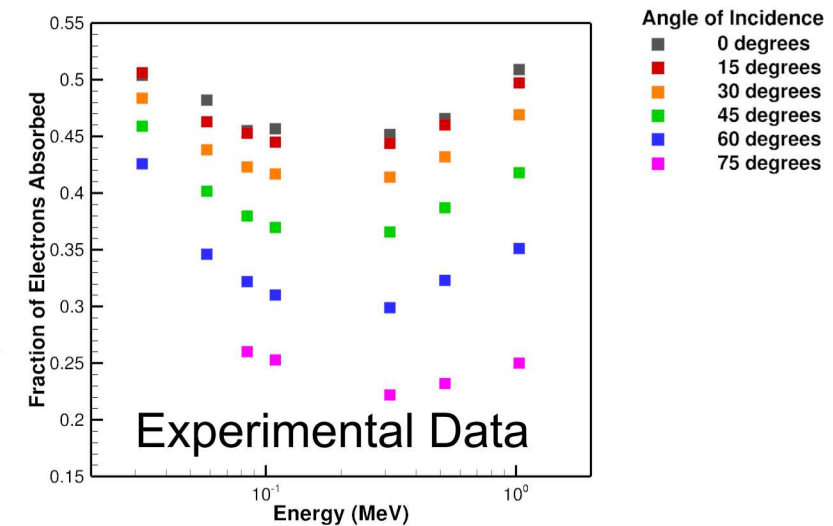
Monoenergetic sources, from 33 keV to 1 MeV

Angles of incidence from normal to 75 degrees

Experiment measured fractional current absorbed

Comments: Slightly higher results from condensed history than from multigroup, which are slightly higher than analog, but generally consistent trends. Poorer agreement at tangential angles and low energy.

Poor agreement for analog above 256 keV.



Hanson Angular Scattering

Electron beam normally incident on a thin foil of gold of $9.658 \mu\text{m}$

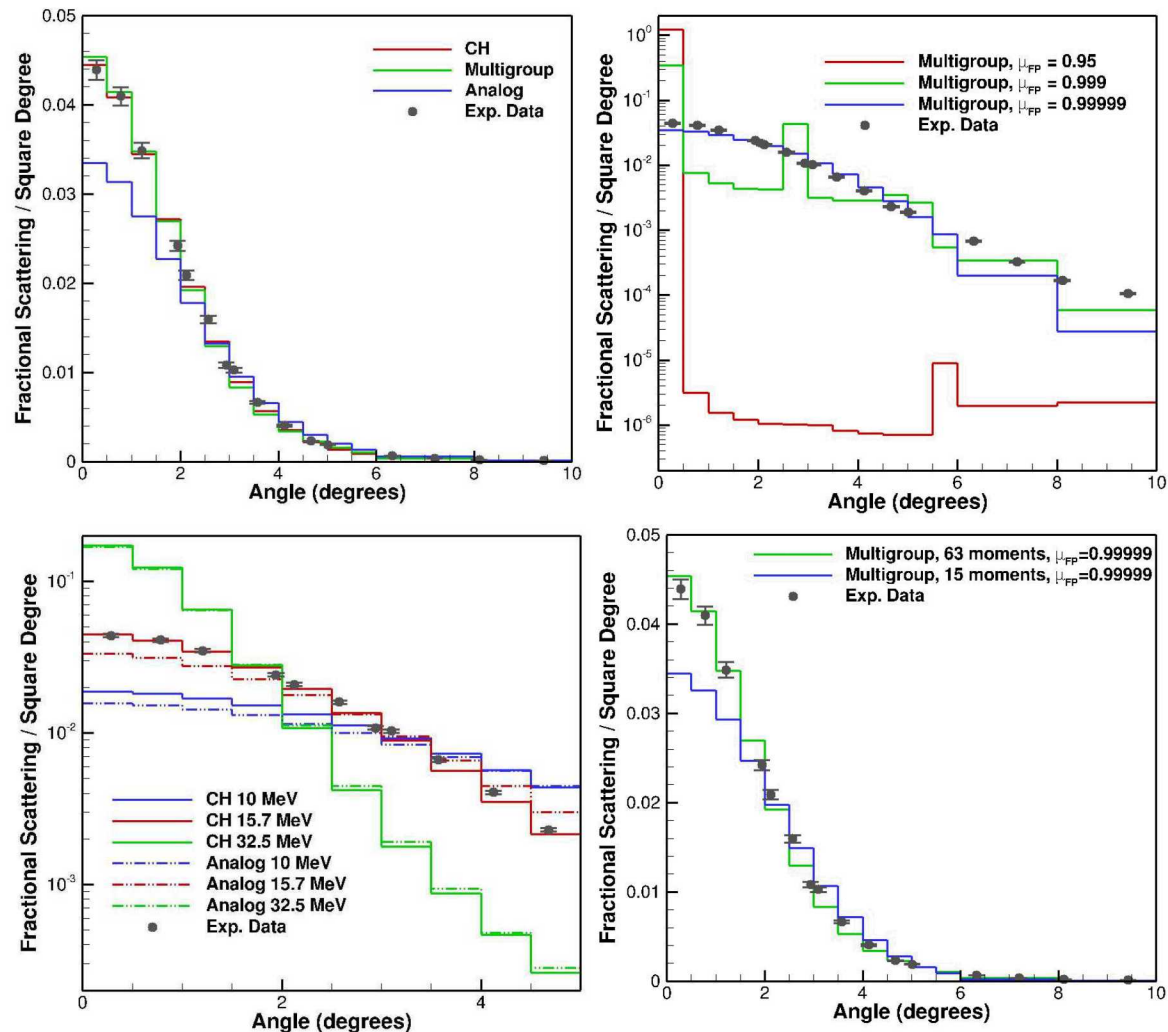
Monoenergetic at 15.7 MeV

Experiment measured angular distribution of transmission

Comments:

Good agreement between condensed history and multigroup with data, but some discrepancy with analog.

Multigroup requires high number of scattering moments and very forward-peaked Fokker-Planck angle. Analog shows disagreement with condensed history at 10 MeV (where distribution is tabulated), but less at 32.5 MeV, so disagreement is not only due to interpolation.



Tabata Charge Deposition

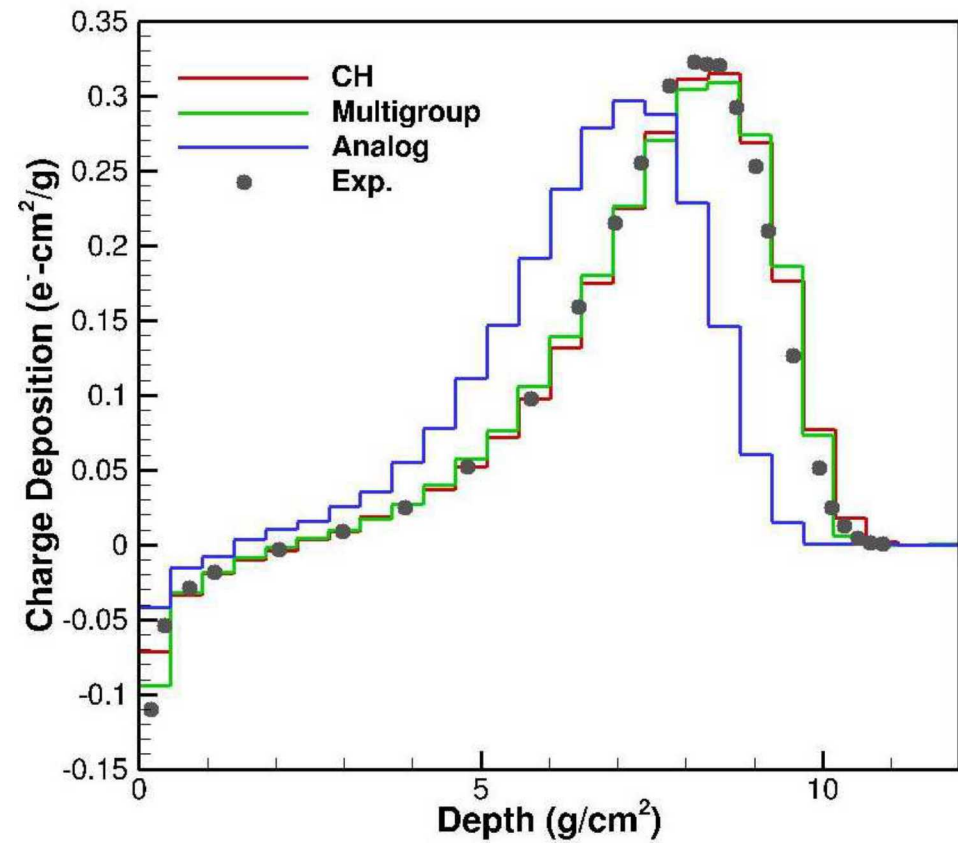
Electron beam normally incident on a thick slab of beryllium

Monoenergetic source at 14.9 MeV

Experiment measured electron charge deposition

Comments:

Good agreement between condensed history and multigroup with data, but some discrepancy with analog.



McLaughlin Energy Deposition

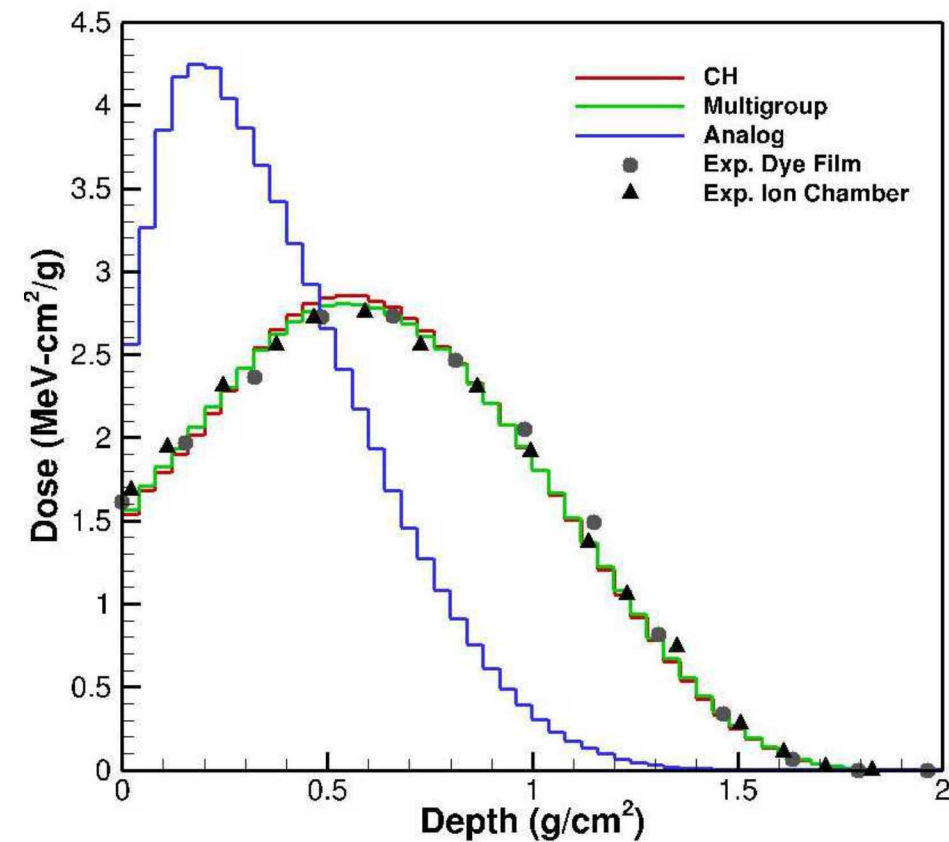
Electron beam normally incident on a thick slab of aluminum

Monoenergetic source at 3 MeV

Experiment measured energy deposition

Comments:

Good agreement between condensed history and multigroup with data, but poor agreement with analog.



Sanford Bremsstrahlung Converter

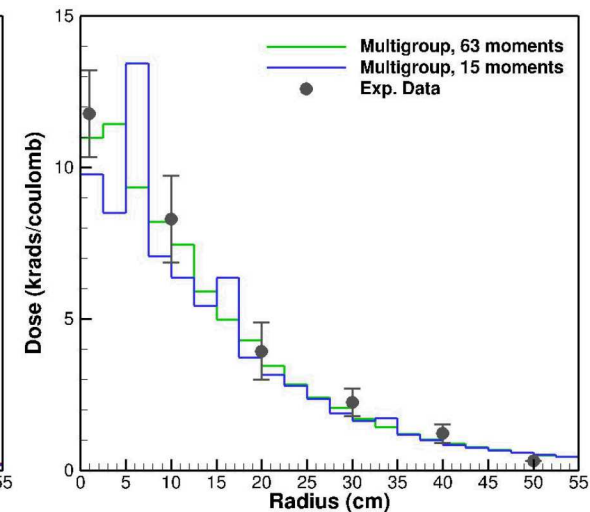
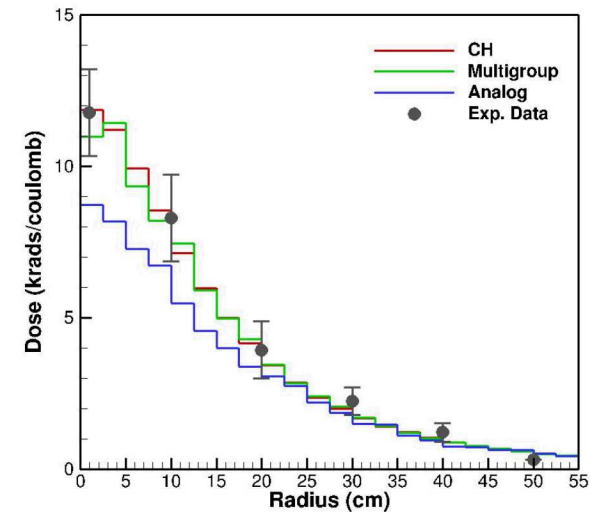
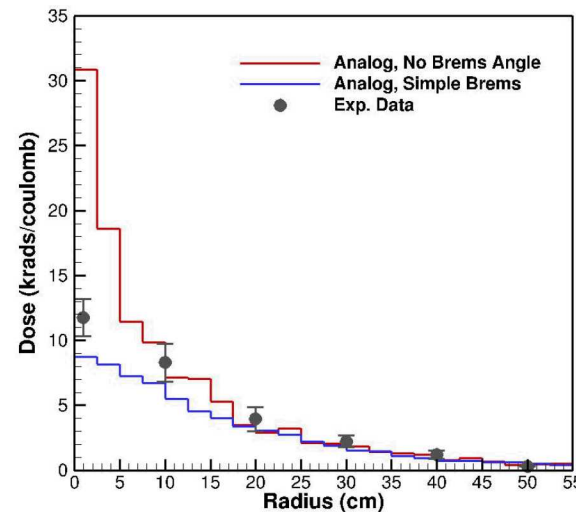
Electron beam incident on a cylinder of carbon cylinder was 1 cm radius and 0.48 cm thick (more than an electron range thick)

Monoenergetic source at 750 keV

Experiment measured dose to TLDs, offset 30 cm down-beam and at various radii

Comments:

Good agreement between condensed history and multigroup with data, but some discrepancy with analog. “Simple brems” model for angular distribution of bremsstrahlung production was needed. Multigroup also uses “simple brems” model, but gives better agreement if sufficient scattering moments are used.



McLaughlin Energy Deposition

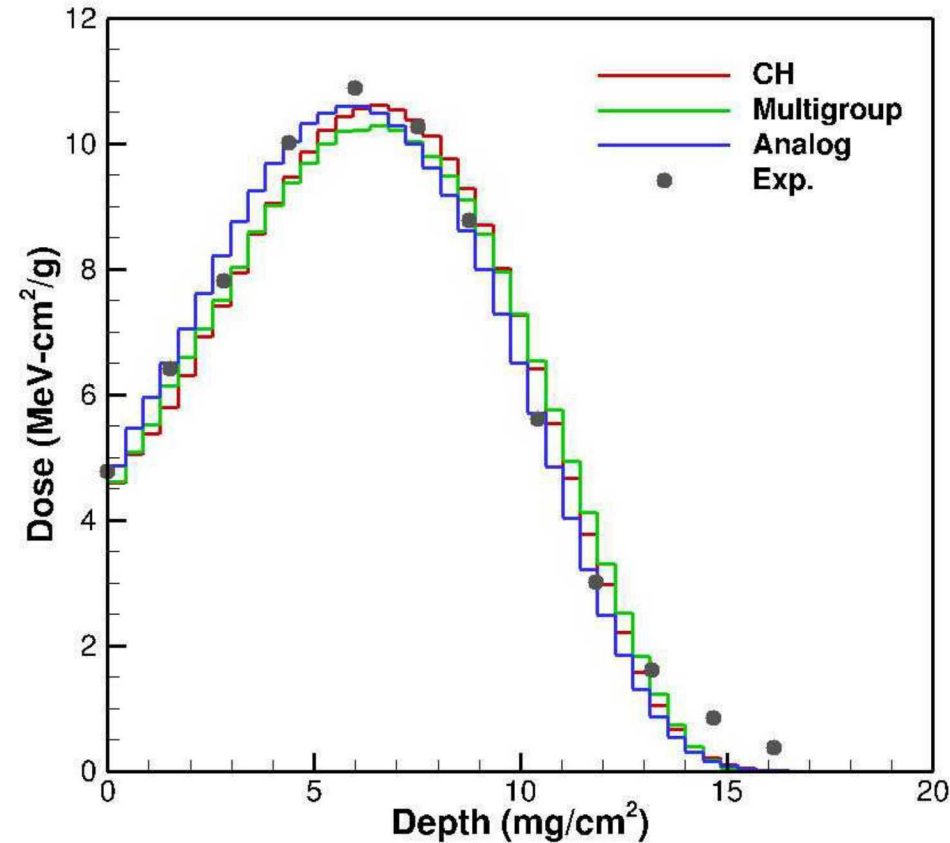
Electron beam incident on thick slab of polystyrene

Monoenergetic source at 100 keV

Experiment measured dose

Comments:

Reasonable agreement between all models and data.

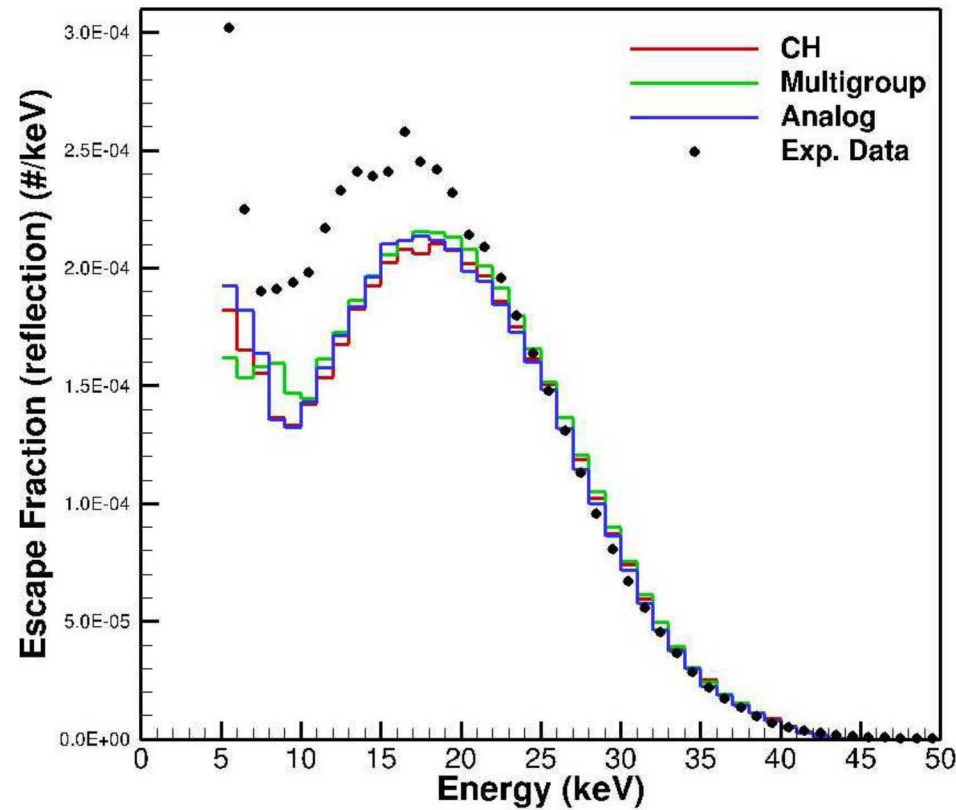


Dolan Photoemission

50 keV endpoint bremsstrahlung source
 Photon spectrum incident on thick slab of tantalum
 Experiment measured reverse electron emission

Comments:

Reasonable agreement between all models and data, though consistent discrepancy at low energy. Differences in relaxation models account for differences in results between the three models below 10 keV.



Relaxation Radiation

Photon beam incident on thick slab of gold

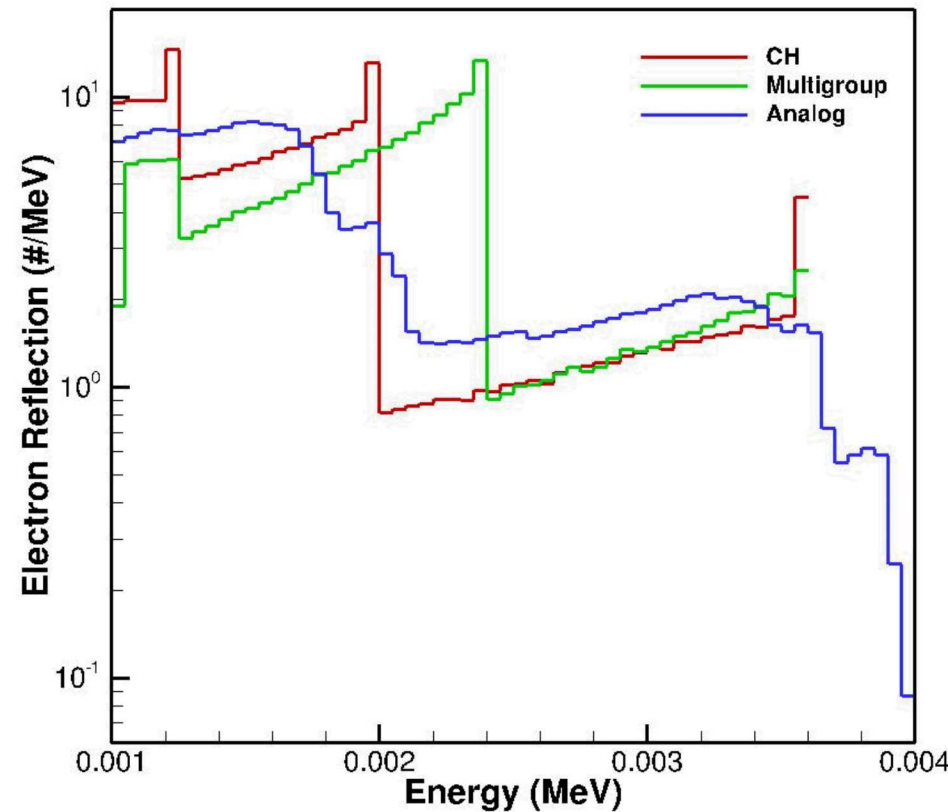
Monoenergetic source at 4 keV

No experimental data, computational comparison only

Reverse electron emission

Comments:

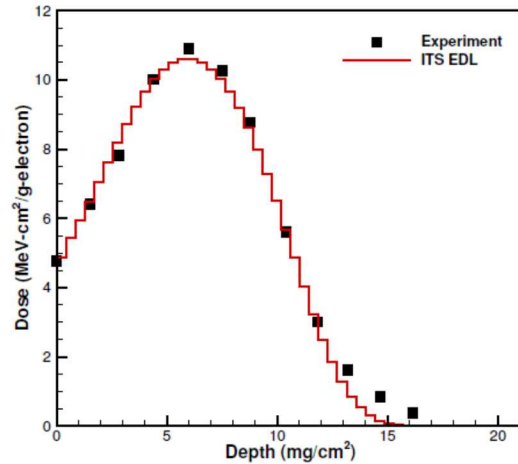
This problem highlights the differences in the relaxation models. The detailed shell model in the analog simulation produces many different fluorescence and Auger line energies.



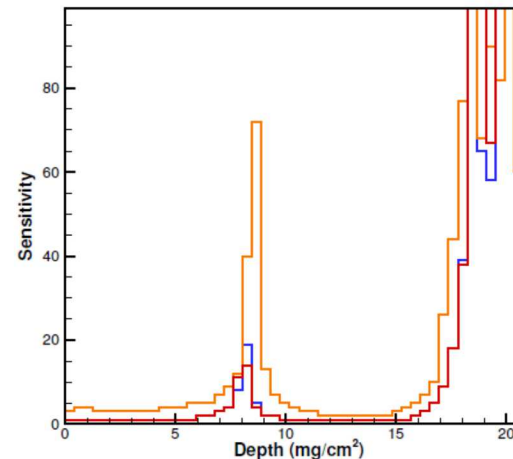
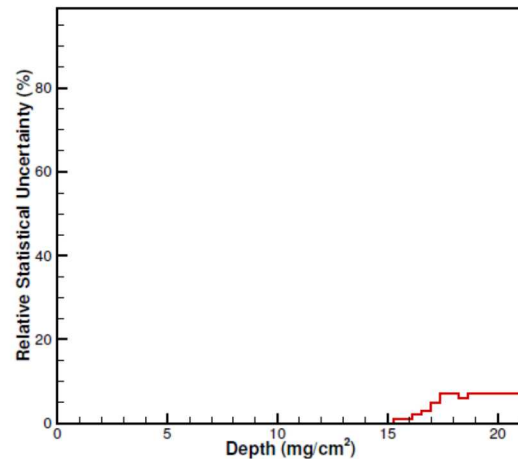
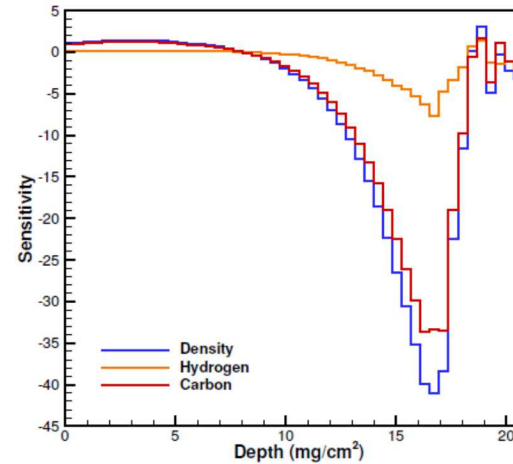
Differential Operator Sensitivity

McLaughlin energy deposition from a normally incident 100 keV electron beam on polystyrene.

Energy deposition vs. Experiment



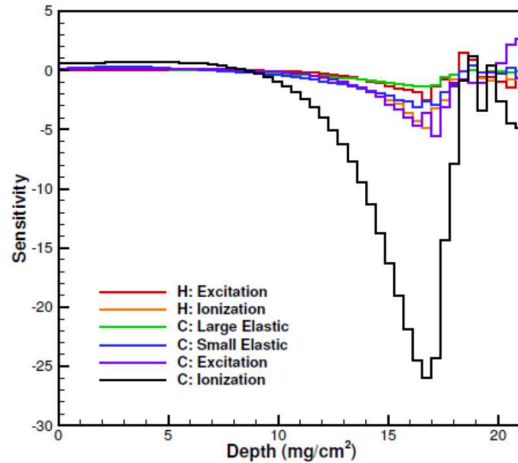
Differential Operator Sensitivities



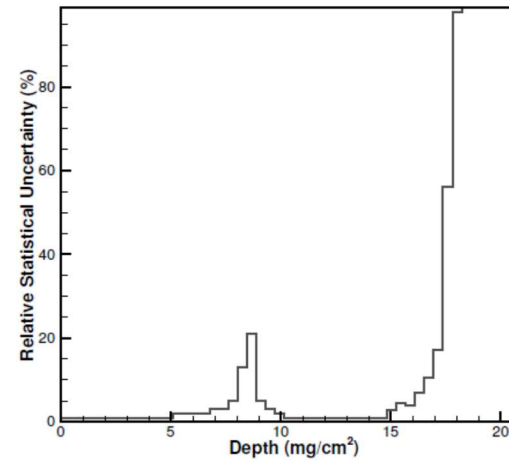
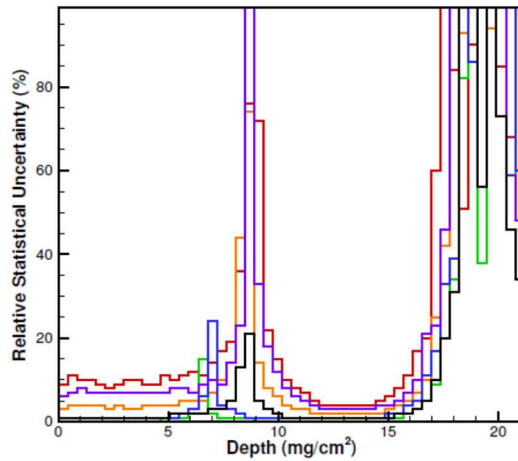
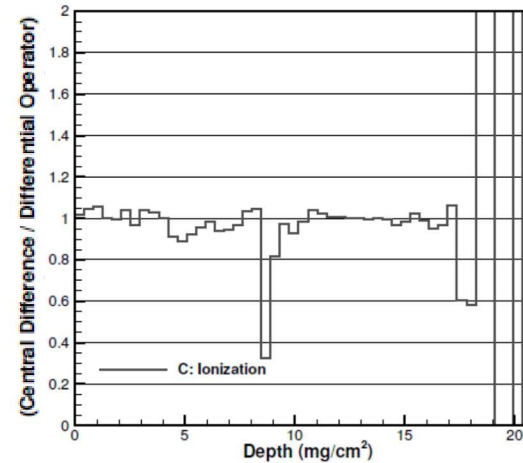
Differential Operator Sensitivity

McLaughlin energy deposition from a normally incident 100 keV electron beam on polystyrene.

Differential Operator Sensitivities

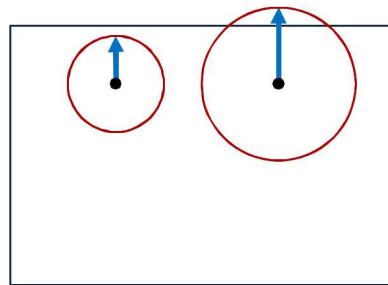


Ratio of DO to CD Sensitivities



Biasing with Electron Trapping

“Electron Trapping” is a truncation method. For electrons below a user-specified threshold energy, the range of an electron is compared to the distance to geometry boundaries (and subzone tally-region boundaries). If the electron cannot reach the boundary, then it is “trapped”. Trapped electrons are terminated, and energy and charge is deposited locally.



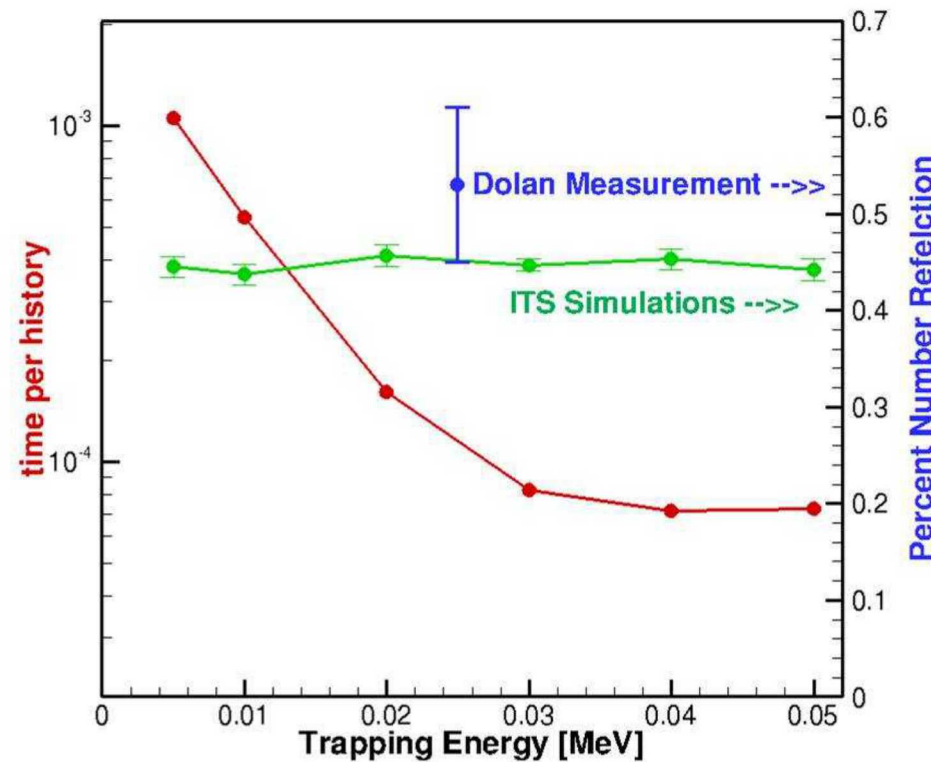
50 keV endpoint bremsstrahlung source

Photon spectrum incident on slab of tantalum

Experiment measured reverse electron emission

Comments:

Electron trapping can dramatically improve run times without significantly affecting the computational result.



Conclusions and Future Work

- Generally, we achieve reasonable agreement with experimental validation data with all three algorithms.
- The limitations in the elastic scattering angular distribution data appear to affect the accuracy of electron transport using the EEDL data for problems above 256 keV.
 - We plan to investigate alternative distributional data, such as from ELSEPA.
- We have added a bremsstrahlung angular distribution model to the analog model.
- For “thin” problems, the multigroup model shows discrete scattering artifacts.
 - Alternative cross section generation settings (that increase the total cross and number of discrete scattering angles) can improve the agreement with validation data.
- Analog is computationally expensive, especially for high energy problems.
 - We will be implementing biasing techniques and moment-preserving GBFP methods to accelerate the transport.